

## DICE Mission Design, Development, and Implementation: Success and Challenges

Chad Fish, Charles Swenson, Tim Neilsen, Bryan Bingham, Jake Gunther,  
Erik Stromberg, Steven Burr, Robert Burt, Mitch Whitely  
Space Dynamics Laboratory/Utah State University  
1695 N Research Park Way, North Logan, UT 84341; (435) 713-3355  
[Chad.Fish@sdl.usu.edu](mailto:Chad.Fish@sdl.usu.edu)

Geoff Crowley, Irfan Azeem, Marcin Pilinski  
Atmospheric & Space Technology Research Associates, LLC  
5777 Central Ave, Ste. 221 Boulder, Colorado 80301; 210-834-3475  
[gcrowley@astraspace.net](mailto:gcrowley@astraspace.net)

Aroh Barjatya  
Embry Riddle Aeronautical University  
600. S Clyde Morris Blvd Daytona Beach, FL 32114; 386-226-6675  
[aroh.barjatya@erau.edu](mailto:aroh.barjatya@erau.edu)

Justin Petersen  
L-3 Communications  
640 N 2200 W, Salt Lake City, UT 84116; 801-594-2000  
[justin.c.petersen@L-3com.com](mailto:justin.c.petersen@L-3com.com)

### ABSTRACT

Funded by the NSF CubeSat and NASA ELaNa programs, the Dynamic Ionosphere CubeSat Experiment (DICE) mission consists of two 1.5U CubeSats which were launched into an eccentric low Earth orbit on October 28, 2011. Each identical spacecraft carries two Langmuir probes to measure ionospheric *in-situ* plasma densities, electric field probes to measure *in-situ* DC and AC electric fields, and a magnetometer to measure *in-situ* DC and AC magnetic fields. Given the tight integration of these multiple sensors with the CubeSat platforms, each of the DICE spacecraft is effectively a “sensor-sat” capable of comprehensive ionospheric diagnostics. Over time, the sensor-sats will separate relative to each other due to differences in the ejection velocity and enable accurate identification of geospace storm-time features, such as the geomagnetic Storm Enhanced Density (SED) bulge and plume. The use of two identical sensor-sats permits the de-convolution of spatial and temporal ambiguities in the observations of the ionosphere from a moving platform. In addition to demonstrating nanosat constellation science, the DICE mission downlink communications system is operating at 3 Mbit/s. To our knowledge, this transmission rate is a factor of 100 or more greater than previous CubeSat missions to date.

This paper will focus on the DICE mission design, implementation, and on-orbit operations successes as well as the challenges faced in implementing a high-return science mission with limited resources. Specifically, it will focus on the lessons learned in integrating, calibrating, and managing a small constellation of sensor-sats for global science measurements.

### INTRODUCTION

The most significant advances in Earth, solar, and space physics over the next decades will originate from new observational techniques. The most promising observation technique to still be fully developed is the capability to conduct multi-point or large, distributed constellation-based observations of the Earth system at a feasible cost. This approach is required to understand the “big picture”--system-level coupling between disparate regions such as the solar-wind,

magnetosphere, ionosphere, thermosphere, mesosphere, atmosphere, land, and ocean on a planetary scale. The NASA Science Mission Directorate has repeatedly identified in recent roadmaps the pressing need for multipoint scientific investigations, to be implemented via satellite constellations<sup>1</sup>. The NASA Earth Science Division’s “A-train”, consisting of Aqua, CloudSat, CALIPSO and Aura satellites, each with different sensors, is an example of such a constellation. However, the costs to date of this and other proposed

constellations have been prohibitive given previous “large satellite” architectures and the multiple launch vehicles required for implementing the constellations.

Affordable multi-spacecraft constellations can only be achieved through the use of small spacecraft that allow for much more modest fabrication, assembly, test, and launch integration infrastructures and processes as well as multiple hostings per launch vehicle. The revolution in commercial mobile and other battery powered consumer technology has allowed researchers in recent years to build and fly very small satellites, namely CubeSats. Recent CubeSat based research initiatives, such as the NSF CubeSat Space Weather and the Air Force Space Environmental NanoSat Experiment (SENSE) programs, have spurred the development of very capable miniature space science sensors that readily integrate into a CubeSat.

In previous Small Sat meetings, the NSF and NASA-sponsored Dynamic Ionosphere CubeSat Experiment (DICE) space weather mission objectives and design have been presented<sup>14,15</sup>. In the current paper, we present much more detail on the mission objectives, design and implementation, and on-orbit performance. This two-spacecraft CubeSat mission exemplifies a next-generation advanced space research undertaking. In addition to having its own specific mission research objectives, it is also intended as a pathfinder to low-cost multi-point CubeSat constellation observations of the Earth system. This paper will also include a review and discussion of the to-date successes, challenges, and lessons learned of the DICE mission.

## MISSION OBJECTIVES

### Science Research

Space weather refers to conditions in space (the Sun, solar wind, magnetosphere, ionosphere, or

thermosphere) that can influence the performance and reliability of space-borne and ground-based technological systems. Ionospheric variability has a particularly dramatic effect on radio frequency (RF) systems; for example, large gradients in ionospheric electron density can impact communications, surveillance and navigation systems<sup>2,3</sup>. Some of the largest gradients are found on the edges of geomagnetic Storm Enhanced Density (SED) features, which regularly occur over the US in the afternoon during magnetic disturbances. The SED feature was first identified by Foster<sup>6</sup> using the Millstone Hill incoherent scatter radar (ISR), although Total Electron Content (TEC) enhancements caused by SEDs had been observed much earlier<sup>4,5,6</sup>. More recently, 2-D TEC maps obtained from global ground GPS receivers have shed new light on the space-time properties of mid latitude SED, and its relationship to plasmaspheric processes<sup>7,8</sup>.

The formation and evolution of SED can be described by two related structures (reference Figure 1). The first is the formation of a greatly enhanced SED “bulge” of plasma which seems to preferentially originate at southern USA latitudes and appears correlated with storm-time prompt penetration electric fields (PPE) at low latitudes<sup>9,10</sup>. The second is the formation and evolution of a narrow SED “plasma plume” that first forms at the base of the SED bulge, and then extends pole-ward into and across the polar cap. The SED plume appears to be strongly correlated with the expansion of the polar convection cells, and is thought by some investigators to be due to the existence of a strong sub-auroral polarization stream (SAPS) in the local afternoon/evening mid-latitude sector<sup>11,12</sup>.

Several important research questions regarding SEDs are still unanswered. First, how exactly the greatly

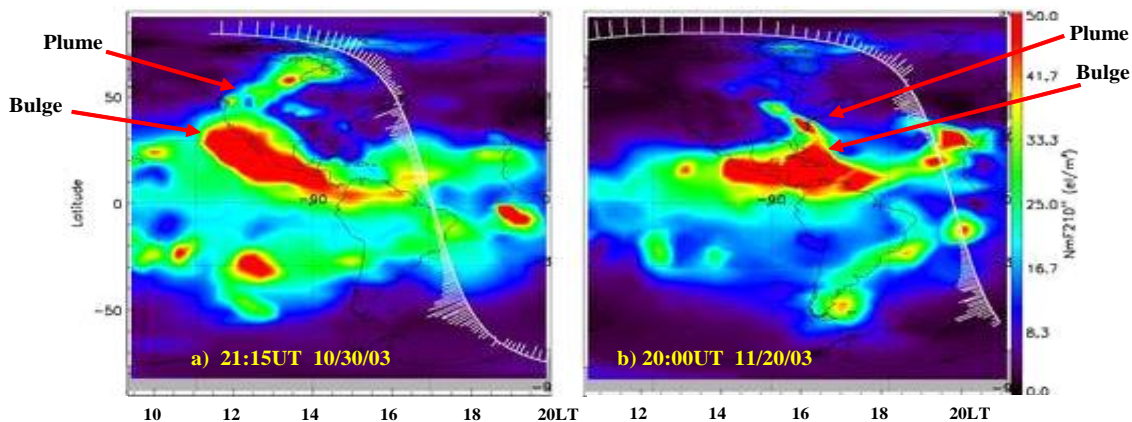


**Figure 1. Horizontal distribution (Latitude vs. Local Time) of F-region peak electron density (NmF2) from IDA4D for: (a) October 30 (b) November 20, 2003. Units are  $1 \times 10^{11} \text{ m}^{-3}$ . DMSP ion drift vectors shown.**

enhanced plasma is formed over the southern USA (the SED bulge) and what is the source of the plasma. Second, exactly what physical drivers are involved in the formation and evolution of the SED plume, and what is their relative importance. Finally, the precise relationship between the occurrence of penetration electric fields (PPEs), the subsequent expansion of the Appleton anomaly crests, and the development of SED is still an open research question, particularly in terms of why there is an apparent preference for the USA geographic sector shown in Figure 1. Ultimately the large redistributions of ionospheric plasma interfere with radio communications and the SED plume causes GPS navigation blackouts for users over North America. Since modern society has come to rely upon radio and more increasingly GPS, the ability to understand and predict space weather effects on these services is of importance.

To address the outstanding questions of SED science, the DICE mission has three main scientific objectives:

1. Investigate the physical processes responsible for formation of the SED bulge in the noon to post-noon sector during magnetic storms.
2. Investigate the physical processes responsible for the formation of the SED plume at the base of the SED bulge and the transport of the high density SED plume across the magnetic pole
3. Investigate the relationship between PPE and the formation and evolution of SED

The DICE science objectives can be achieved via *in-situ* ionospheric electric field and plasma density measurements from a multi-spacecraft mission. The electric field and plasma density measurements allow for the characterization of both the ionospheric plasma density and the electric field distribution. Ideally what is needed to study SEDs is a set of simultaneous co-located plasma density and electric field measurements passing through the SED bulge and plume in the afternoon sector as they start to develop and then as they evolve. Thus the DICE satellites should sample the afternoon sector between ~ 13-17 LT, where they will observe important features that have never been seen. With two spacecraft, it is possible to begin to separate temporal and spatial evolution of the SEDs. The two DICE spacecraft will drift apart in latitude over the life of the mission, so that they see the same plasma at slightly different times (time evolution).

SEDs are large-scale features; therefore high time-resolution is not required for the measurements. The electric fields causing the SED bulge and plume have similar scales. With an approximate spacecraft velocity of 7 km/sec a spacecraft will take approximately 7-14 seconds to traverse the SED plume, therefore a cadence of 0.5 to 1 seconds for the plasma and electric field measurements is sufficient to define the SED plume and the related (broader) plasma electric field structures. Although not the focus of the DICE mission, ionospheric irregularities are of great interest for space

**Table 1. Science to Mission Functionality Requirements Traceability Matrix**

<b>Science Objective 1: Investigate formation of the SED bulge over the USA</b>		
<b>Measurement Req.</b>	<b>Instrument Req.</b>	<b>Mission Req.</b>
<b>Measure RMS Fluctuations in Electric Field and Plasma Density:</b> 1. Make co-located DC electric field and plasma density measurements at a $\leq 10$ km on-orbit resolution 2. Make AC electric field measurements at a $\leq 10$ km on-orbit resolution 3. Make measurements on a constellation platform of $\geq 2$ spacecraft that are within 300 km	<b>Electric Field:</b> 1. Max range of $\pm 0.6$ V/m 2. Min threshold of 0.6 mV/m 3. Min resolution of 0.15 mV/m 4. DC sample rate $\geq 4$ Hz 5. AC sample rate $\geq 4$ kHz [Telemetry AC FFT power information at $\geq 1$ Hz (3 points)] <b>Plasma (Ion) Density:</b> 1. Range of $2 \times 10^9$ - $2 \times 10^{13}$ m <sup>-3</sup> 2. Min resolution of $3 \times 10^8$ m <sup>-3</sup> 3. Sample rate $\geq 1$ Hz	1. Constellation size $\geq 2$ satellites 2. Spacecraft spin axis aligned to geodetic axis to within $10^\circ$ ( $1\sigma$ ) 3. Spacecraft spin stabilized to within $1^\circ$ ( $1\sigma$ ) about principal spin axis 4. Spacecraft knowledge to within $1^\circ$ ( $1\sigma$ ) 5. Constellation time synch knowledge $\leq 1$ s 6. Orbital insertion inclination between $55^\circ$ - $98^\circ$ (ideally sun-synchronous at 13-17 LT) 7. Orbital altitude including ranges between 350 - 630 km 8. Spacecraft $\Delta V$ speed of $\leq 50$ km/month 9. Storage/downlink $\geq 31$ Mbits/day. 10. Lifetime $\geq 6$ months
<b>Science Objective 2: Investigate formation of the SED plume over the USA</b>		
<b>Measurement Req.</b>	<b>Instrument Req.</b>	<b>Mission Req.</b>
Same as Science Objective 1	Same as Science Objective 1	Same as Science Objective 1 (downlink included in Objective 1)
<b>Science Objective 3: Investigate correlation of PPE with formation and evolution of SED</b>		
<b>Measurement Req.</b>	<b>Instrument Req.</b>	<b>Mission Req.</b>
Same as Science Objective 1	Same as Science Objective 1	Same as Science Objective 1 (downlink included in Objective 1)

weather. Further, it has been shown that small scale irregularities form on the edges of large SED gradients<sup>4</sup>. The physical instability mechanism is not known, so directly measuring small scale electric fields in association with larger scale SEDs will be quite valuable. The irregularity spectrum will also be captured by the DICE mission in terms of the AC electric field spectrum measurements. In addition, observations at the Millstone Hill ISR have shown small scale electric field variability associated with the larger scale SAPS channel<sup>12</sup>. It is possible that there is a physical connection between small scale AC electric field variability and the larger scale dynamics of the SED plume development right on the edge of the large scale gradient field.

The DICE science objectives to instrument and mission performance requirements are shown in Table 1. The three science objectives for the DICE mission are listed and correspond to questions about the SED bulge and plumes, their formation and motion. Table 1 also lists the minimum required measurement parameters of electric fields and density and basic instrument requirements for the investigation including the range and minimum sensitivity level for each science objective as determined by the DICE science team.

### ***Technology Demonstration***

Perhaps the most pressing enabling technology for CubeSats is the ability to down-link large amounts of data to the ground. In addition to its science research objectives, DICE also has a major technology demonstration objective; namely to demonstrate a reliable high-speed communication downlink on non-amateur radio band from a CubeSat. This objective was identified early in the program as key to promoting and progressing the use of CubeSats, and small satellites in general, for low-cost access to space to implement multi-point measurements of the Earth system. Based on previous space flight mission experience, the DICE team determined that a CubeSat telemetry downlink capability > 1 Mbit/s would be a significant leap forward from the technology existent at the time of the DICE mission inception and would enable major research constellation missions by providing the needed bandwidth for desired measurements.

A high speed downlink requires significant spectral bandwidth and the relevant frequencies for regular non-experimental space-to-earth communications in which large bandwidths can be allocated are at UHF (460-470 MHz, 10 MHz allocation) and S-Band (2200-2290 MHz, 5 MHz allocations). The greatest difficulty in developing new communication technologies for small spacecraft is working within the regulatory framework

as plumaged by the United Nations through the International Telecommunications Union (ITU) and the National Telecommunications and Information Administration (NTIA) within the United States. DICE wanted to make use of radio bands approved by the NTIA for government use in the application of space-to-earth and earth-to-space communication systems. Because the radios ultimately developed for use on DICE would be in regularly licensed bands they could then be rapidly infused into the conservative space-user community.

### ***Broader Impact***

As an NSF and NASA Educational Launch of Nanosatellites (ELaNa) sponsored CubeSat program, a key educational objective of the DICE program is that it be implemented and executed by university undergraduate and graduate students from a broad range of disciplines, under mentorship and supervision of professional staff and faculty. This objective is motivated by the desire engage, inspire, and provide training for the next generation of engineers and space scientists.

Additionally, the DICE team felt strongly that low-cost, reliable research and operational CubeSat-based missions would most readily become viable if a strong technical collaboration, based on common goals, was developed and fostered between small business, academia, government, and industry. The DICE team identified two areas which they feel are strategic to long term CubeSat mission success as well as being suitable for multi-institution partnering. Those areas, which became DICE mission teaming objectives, are:

1. Development of high-speed downlink communications for use on regularly licensed bands. This would include not only the design and implementation of a high-speed space to ground radio, but also the tools, facilities, and infrastructure to provide the ground tracking, comm link closure (i.e., high-gain ground antenna to enable the high-speed downlink), and data acquisition and management on the ground.
2. Development of miniature, reliable CubeSat deployment mechanism transducers. This refers to the need for transducers such as wax or shape-memory alloy actuators that can operate within a CubeSat power budget and only occupy a very small percentage of a CubeSat volume.

## DESIGN AND IMPLEMENTATION



**Figure 2. The DICE mission is a next-generation NSF and NASA-sponsored space research mission formed around CubeSat technologies.**

### Team Organization

The DICE Principal Investigator is Geoff Crowley from ASTRA Inc. Charles Swenson, Space Dynamics Lab/Utah State University (USU/SDL), is the Deputy Principle Investigator. The DICE program was implemented at USU/SDL and mission operations are conducted by USU/SDL in collaboration with NASA Wallops Flight Facility and SRI International. Science co-Investigators include Marcin Pilinski and Irfan Azeem from ASTRA, Aroh Barjatya from Embry Riddle University, and Miguel Larsen from Clemson University. The project lead engineer is Tim Neilsen, SDL/USU. Major industry partners include L-3 Communications, TiNi Aerospace, Clyde Space, ATK, and Pumpkin Inc. GPS simulator testing occurred in collaboration with the NASA Goddard Space Flight Center.

### Sensor Sat

The design of the DICE sensor-sats is the result of a number of drivers and requirements including:

1. Provide a science and technology pathfinder demonstration to progress future CubeSat based constellation missions,

2. The DICE science and technical demonstration mission objectives,
3. Limited funding resources (~ \$1 M) to build, test, launch, and operate the spacecraft, and
4. Conformance to P-POD containerized launch system for secondary payloads of 10 x 10 x 30 cm in volume and 4 kg in mass

The major science objective driver was the need to deploy electric field sensors a number of meters in length from the spacecraft to make the electric field measurements. Additionally, they need to spin regularly about a controlled axis such that observational errors (e.g., DC offsets and  $\mathbf{v} \times \mathbf{B}$  induced emf) can be identified and removed from the data. This requires a method to store a pair of lengthy booms from a compact volume (9.5 x 9.5 x 1.5 cm) which could later be released to their full length. A secondary science objective required the Langmuir probes to be placed away from the spacecraft. This required a spring loaded boom or 'scissor' booms to accomplish this task.

The DICE spacecraft are comprised of two 1.5U CubeSats, affectionately named Farkle (or DICE1) and Yahtzee (or DICE2). Each identical spacecraft carries two electric field probe pairs to measure *in-situ* DC and AC electric fields, two Langmuir probes to measure ionospheric *in-situ* plasma densities, and a complementary science grade magnetometer to measure *in-situ* DC and AC magnetic fields (see Figure 3, top panel). The four electric field booms each extend 5 m from the spacecraft with electrically conductive spheres on the ends of the booms. The four shorter booms on the bottom-side of the spacecraft comprise the UHF communications turnstile antenna and are 0.2 m in length. The UHF booms also increase the moment of inertia for the controlled spin of the spacecraft about the desired axis. The Langmuir probe spheres are supported on the top and bottom of the spacecraft by the use of scissor booms that extend 8 cm away from the spacecraft. The bottom Langmuir probe boom, as well as the bottom spacecraft panel, supports placement of a science grade magnetometer. Given the tight integration of these multiple sensors within the CubeSat platform, each of the DICE spacecraft is effectively a "sensor-sat" capable of comprehensive ionospheric diagnostics.

Each sensor-sat consists of a frame manufactured from a single block of 7075 Aluminum. An isogrid pattern was used to maintain structural integrity while reducing the mass of the structure. By using a single piece of aluminum, the structure is inherently stiff. The top and bottom panels (+Z and -Z faces) are also machined



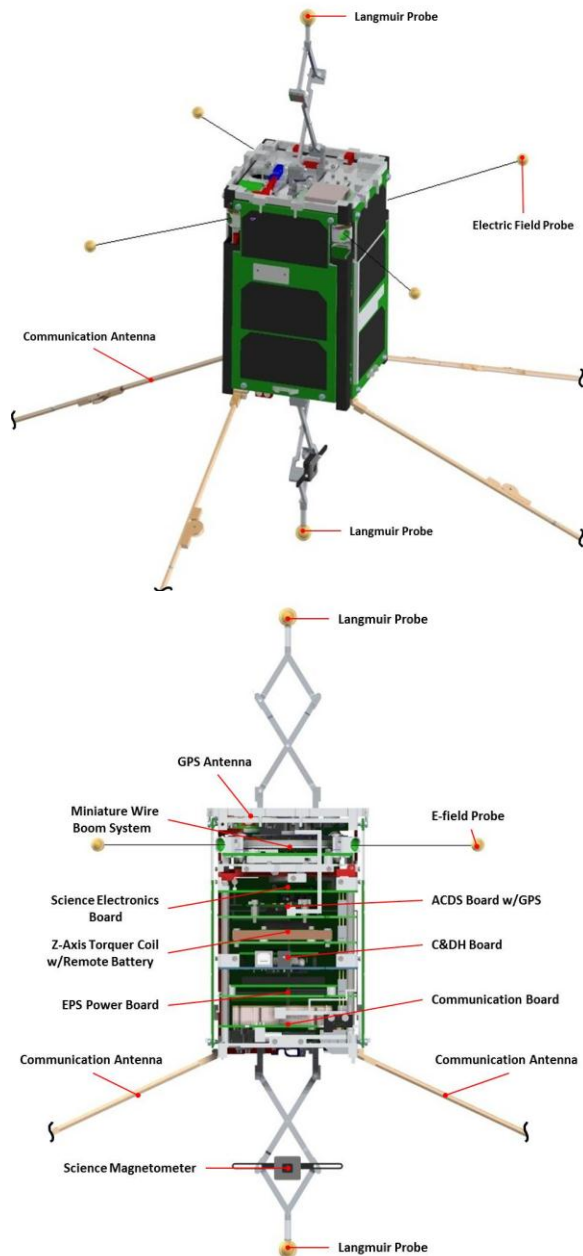


**Figure 3. (Top panel) The DICE sensor-sat configuration (note, electric field booms only shown in partially deployed state). (Bottom panel) Cut-away view of the spacecraft showing the tightly integrated components, sensors, and electronics.**

aluminum, with cutouts and mounting holes for release mechanisms, the Langmuir probes, GPS antenna, science magnetometer, and antenna mounts. Electronics are mounted in a vertical stack (reference Figure 3, bottom panel), and consist of, moving from the bottom of the stack up, 1) radio (L-3 CadetU) and antenna interface components, 2) electrical power system (EPS)

that includes batteries, solar panel connections, and power system monitoring and conditioning, 3) control and data handling (C&DH) electronics, 4) Z-axis torque coil components, 5) attitude control and determination system (ADCS) electronics that include interfaces to a suns sensor, ADCS magnetometer, GPS receiver, and the spacecraft torque coils (Z-axis in stack, X- and Y-axis embedded in solar panel circuit boards), and 6) science electronics that include interfaces to the electric field, Langmuir probe, and science magnetometer sensors. The electric field boom deployment mechanism is mounted above the electronics stack and the main release mechanism for the antennas and scissor booms. The GPS antenna is located on the top panel. Solar panels with three solar cells each are attached on the long sides. A sun sensor “looks out” a small cut out in one of the solar panels. An attitude determination magnetometer is located on the ADCS electronics board within the spacecraft. The use of magnetic materials was avoided in the design of the DICE spacecraft to minimize magnetic contamination of the science magnetometer measurements. The DICE sensor-sat instrumentation map, in spacecraft body coordinates, is shown in Figure 4.

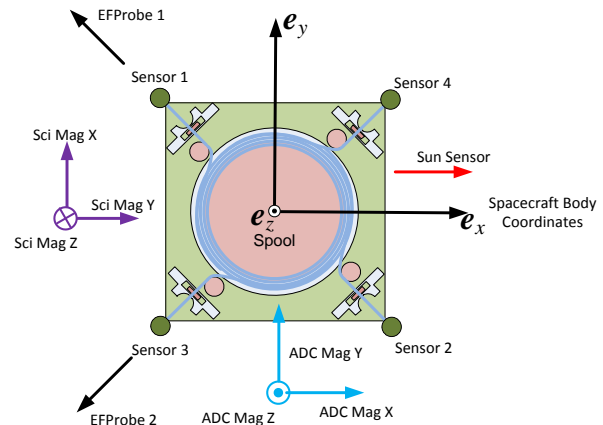


**Figure 4. The DICE sensor map indicates the relative geometry between the ADCS and science measurement components, based on the spacecraft body coordinates.**

The DICE sensor-sats principally use passive thermal control. Survival heaters for the batteries are the only active thermal control on the CubeSat. The solar panels are isolated from the spacecraft body, reducing the internal temperature swing due to solar radiation. The radio dissipates a significant amount of power during its relatively short transmit duty cycle, and has a direct thermal conduction to the bottom exterior panel, which serves as a radiator. This panel has a silverized FEP coated surface for optimum emissive properties.

Temperature sensors are located on key components of the spacecraft.

The main release mechanism, which secures and releases the Langmuir probe scissor booms and UHF antennas, is comprised of a spring loaded lever that runs from the top to the bottom of the CubeSat. It translates along the  $-X$  axis to release both of the Langmuir probes, the antennas, and removes the first mechanical lock on the E-field spool. This mechanism is released by a shape-memory alloy Frangibolt locking actuator developed by TiNi Aerospace. The UHF antenna extensions, consisting of segments of brass tube and tungsten rod inserts provide additional mass “away” from the spacecraft to enhance spin stability about the  $Z$  axis (long axis) of the spacecraft.

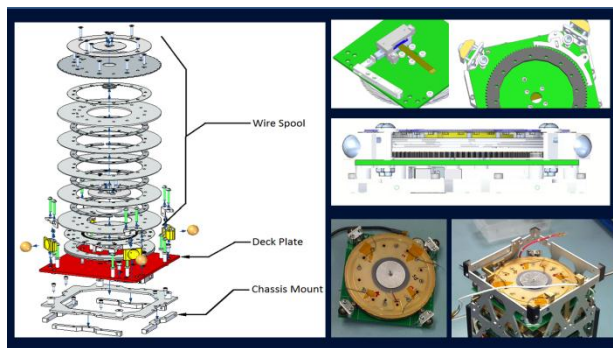


**Figure 5. The DICE electric field boom deployment mechanism includes of a set of precision spools, specialized cabling and harnessing, and non-magnetic motor actuator to deploy 5 m booms on orbit from spinning nano- and pico-satellite platforms.**

The electric field boom deployment mechanism (see Figure 5) provides the means to stow the lengthy 5 m electric field booms during launch and to control their slow deployment during on-orbit operations. Proper deployment of the booms on-orbit is a process that involves balance between centrifugal, centripetal, mechanical friction, motor stepping, and dampening forces acting on the booms while maintaining a stable deployment platform from the spacecraft. A ridged body spinning about the largest of its principal moments of inertia (major axis spinner) is in the lowest energy state possible for its rotational motion and therefore robustly stable. In this state, a spacecraft slowly spins down due to energy loss mechanisms of which the largest is expected to be eddy currents interacting with the Earth’s magnetic field. The response of a ridged body to an external torque applied perpendicular to the angular momentum is a shift of the instantaneous rotation vector resulting in the well-

known coning or precession of the body axis in space about the angular momentum vector. This type of motion implies that the spacecraft has additional energy above the lowest energy state. Over time this energy will be dissipated, principally through slight flexures of the various booms, until the spacecraft returns to the minimum energy state with simple spinning motion about the major axis of inertia.

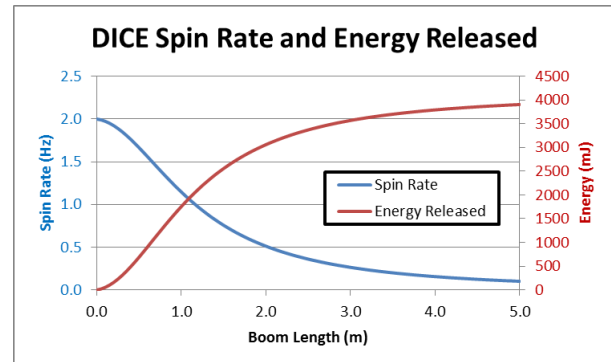


**Figure 6. The DICE spacecraft spin rate will decrease as the wire booms are deployed. Energy will be freed in the system as the booms are deployed.**

The deployment of the DICE electric field wire booms will be done gradually, over time and in stages such that the rotational motion of the spacecraft and wire booms are stable. This will be guaranteed by keeping the spacecraft close to the minimum energy state throughout the deployment process. These procedures will avoid large oscillations of the system, particularly large pendulum motions of the wire booms due to the simple concept that there is not enough free energy in the system to allow such motions to occur. All four electric field sensors will be deployed on wire booms simultaneously via unwinding from a common spool. An incremental extension of the wire booms increases the principal moment of inertia of the spacecraft system and thus decreases the spin frequency due to conservation of angular momentum. The minimum energy state of the system also decreases with the larger inertia leaving an incremental amount of energy in the system. This excess energy, or free energy, is expected to result in small excursion pendulum motions of the wire booms within the spin plane of the spacecraft. Coupling processes through geometric misalignment of the boom system with the spacecraft or through dynamic spin imbalances may result in slight coning of the spacecraft body and small out of plane oscillations of the wire booms over time. The magnitude of all oscillations must be bound by the amount of free energy within the system which will dissipate due to energy loss mechanisms. Depending on the wire boom

release mechanism design and its function, some amount of the excess energy will be initially dissipated as work against this release mechanism. The remaining energy becomes the free internal energy of the system and manifests as pendulum oscillation of the wire booms and coning motion of the spacecraft. This free energy will be largely dissipated at the attachment site of the wire booms to the spacecraft.

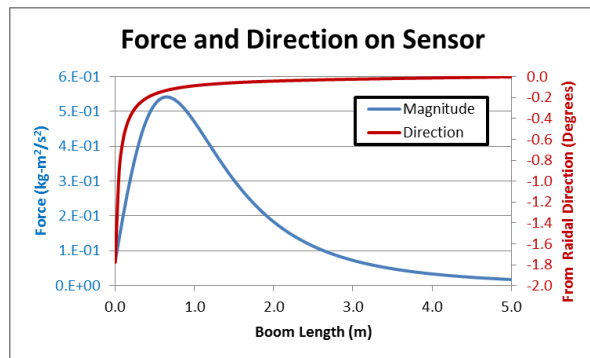


**Figure 7. The magnitude of the forces and the angle from radial of the force acting on the DICE wire boom sensors assuming a constant radial velocity of 1-cm/s and conservation of angular momentum.**

As the wire booms on DICE are deployed, the final moment of inertia for DICE is larger than the initial moment of inertia and energy is transformed in the system. This energy will initially appear as either 1) heating of the deployment mechanism, 2) oscillation of the booms or 3) coning of the spacecraft body. Over time energy dissipation effects will convert it all to heat and the spacecraft is left in a stable spin about the major axis of inertia as illustrated in Figure 6. DICE will initially be spun up to 2 Hz and then the wire booms will be slowly deployed at a rate much slower than 1 cm/s such that the internal energy dissipation mechanisms can dissipate the free energy. The peak tensile force within the wire booms increases initially as the wire booms are deployed and then drops as the booms reach their full extent as illustrated in Figure 7. The direction of the force acting on the booms is essentially radial at slow deployment rates.

### Spacecraft Command, Control, and Operations

A block diagram of the DICE operational sensor-sat sub-systems is shown in Figure 8. The C&DH sub-system, which runs the Pumpkin Inc. Salvo real time operating system (RTOS) on a Pumpkin PIC24 processor card, is the central means by which the spacecraft functions and is controlled. The C&DH sub-system ensures that the spacecraft is operating nominally, responds to warnings or errors, organizes acquisition of housekeeping data, and organizes

acquisition of and compresses data from the science payload. The C&DH also manages transfer of all spacecraft data to the radio for storage and downlink at specified times. Both the radio and payload can be reset from the C&DH. Uplinked commands received by the radio are forwarded on to the C&DH sub-system for execution. Primary means of keeping spacecraft event and measurement time are through a software based clock located in the C&DH. This master clock synchronizes with on-orbit GPS time locks. A secondary crystal based clock is located on the science payload electronics and time codes from this clock are embedded in the science measurements. Spacecraft ephemeris data is passed onto the C&DH from the GPS receiver and included in the DICE downlink telemetry.

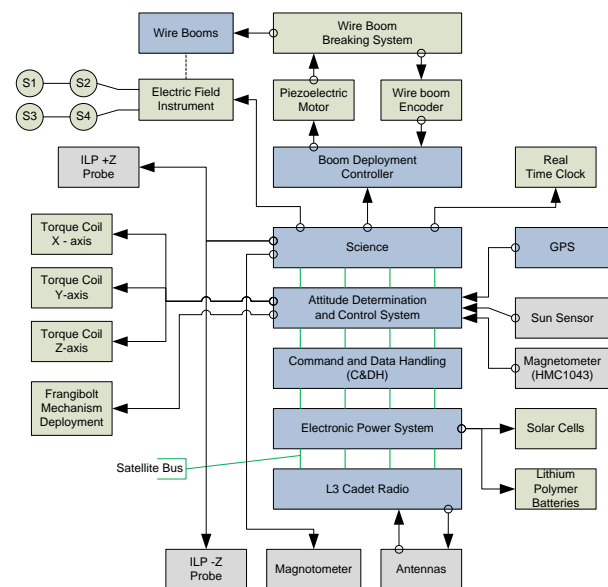


**Figure 8. The DICE sensor-sat is a tightly coupled set of sub-systems that are controlled and managed via the C&DH.** (Note that “ILP” is the Langmuir Probe)

The flight software (FSW) on DICE is implemented with the Pumpkin Inc. Salvo RTOS for all flight software operations. Salvo is a simple, cooperative RTOS which provides event-driven, priority-based multitasking as well as, inter-task communications and synchronization. The flight software (FWS) is comprised of a set of Salvo tasks, each with a distinct function. The DICE flight software block diagram is shown in Figure 9. All communication between tasks occurs using Salvo messages and message queues. These messaging facilities involve using pointers to data structures in memory. Each pointer can be sent as either a simple “message” from one task to another or inserted into “message queue”. At any given time, there can be multiple messages in a single message queue. In the FSW, each message queue will only be



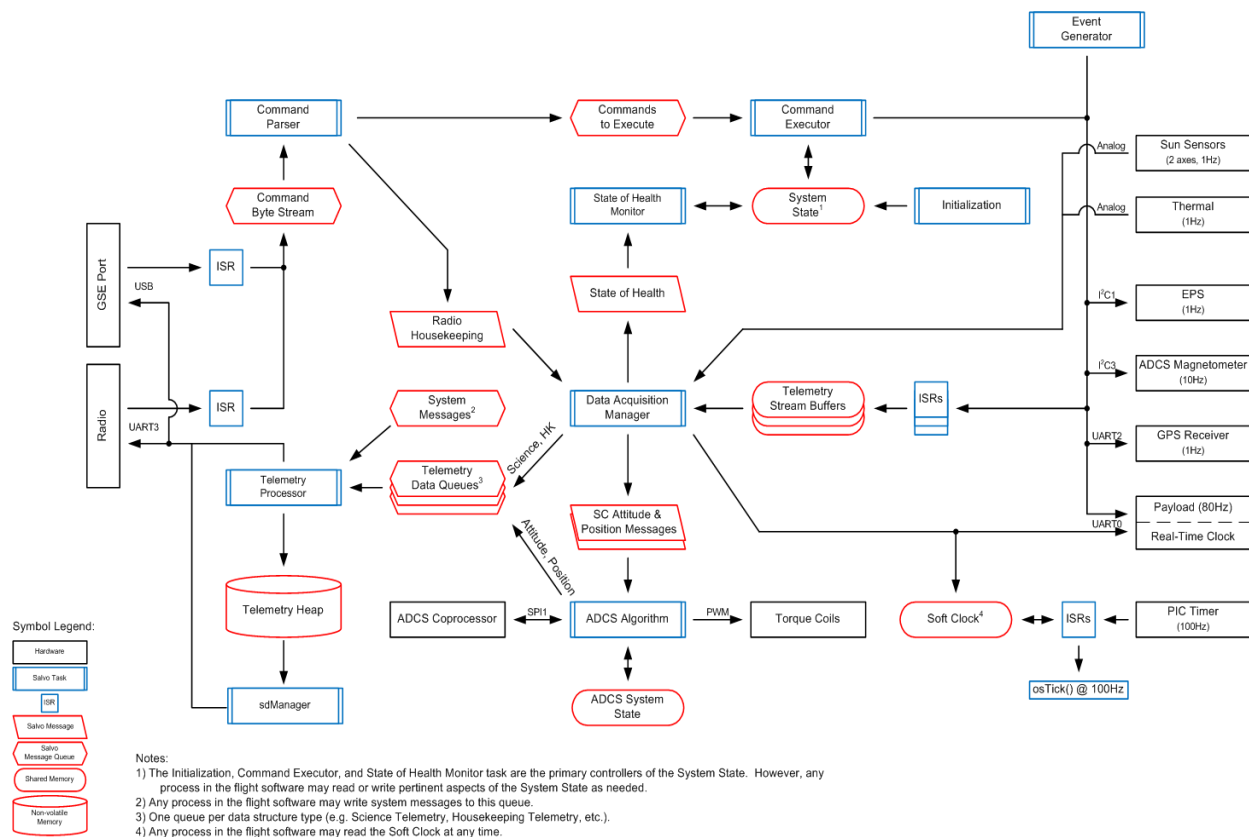


**Figure 9. The magnitude of the forces and the angle from radial of the force acting on the DICE wire boom sensors assuming a constant radial velocity of 1-cm/s and conservation of angular momentum.**

read from by a single task. Typically, each message queue will also be written to by a single task with a few exceptions (e.g. the *System Messages Queue* may be written to by any task).

The FSW implements three distinct spacecraft modes: Safe, Standby, and Operational. The current spacecraft mode affects which spacecraft functions and uplink commands are currently acceptable. The spacecraft boot into Safe mode. The allowed functions in each mode are:

- **Safe Mode**

- Boot to this mode
- Deploy UHF Antennas/Langmuir probes
- Collect ADCS and HK telemetry
- Subsystems unnecessary for spacecraft survival and ground communications are powered down (GPS receiver, payload, torque coils etc. disabled)
- Transition to Standby mode must be commanded by ground

- **Standby**

- Collect ADCS and HK telemetry

- Power to GPS receiver, torque coils allowed
- Transition to Operational mode must be commanded by ground
- State of health monitors or ground command can automatically return the spacecraft to Safe mode

- **Operational**

- Collect Science, ADCS and HK telemetry
- Power to payload, GPS receiver, torque coils allowed
- State of health monitors or ground command can automatically return the spacecraft to Standby or Safe mode

ORBITAL PROPAGATOR	MAGNETIC FIELD MODEL	SUN VECTOR	TRIAD ALGORITHM	OMEGA	CONTROLLER	DETUMBLE
<u>Inputs:</u>	<u>Inputs:</u>	<u>Inputs:</u>	<u>Inputs:</u>	<u>Inputs:</u>	<u>Inputs:</u>	<u>Inputs:</u>
GPS Position	Modified Julian Date	Modified Julian Date	Magnetic Field in Inertial Coordinates	9x9 matrix from Triad	Angular Velocity	Measured Magnetic Field from Magnetometer
GPS Velocity	Results of Orbital Propagator in Earth Fixed Coordinates		Sun Vector	One iteration old 9x9 matrix from Triad	9x9 Matrix from Triad	
			Measured Sun from Sun Sensors		Measured Magnetic Field from Magnetometer	
			Measured Magnetic Field from Magnetometer			
<u>Purpose:</u>	<u>Purpose:</u>	<u>Purpose:</u>	<u>Purpose:</u>	<u>Purpose:</u>	<u>Purpose:</u>	<u>Purpose:</u>
Continues propagating our location in Orbit after the GPS has been turned off.	Calculates the magnetic field based off the inputs given.	Compute sun vector.	Compute 9x9 attitude matrix.	Compute angular velocity.	Compute the desired torque voltages to pulse to the torque coils.	Detumble the X & Y axis of the spacecraft and spin up the Z axis in order to obtain a GPS lock and begin controlled spin.
<u>Outputs:</u>	<u>Outputs:</u>	<u>Outputs:</u>	<u>Outputs:</u>	<u>Outputs:</u>	<u>Outputs:</u>	<u>Outputs:</u>
Position in Inertial Coordinates	Magnetic Field in Earth Fixed Coordinates	Sun Vector	9x9 matrix	Angular Velocity	Desired Torque Voltages.	Desired torque voltages.

**Panel 1. DICE ADCS algorithm definitions, state definitions (Detumble and Controller), and associated, input and output parameters listing.**

### *Spacecraft Electrical Power Systems*

The Clyde Space EPS is comprised of a monitor and control board, lithium-ion batteries, and custom solar panels that include torque coil windings. The EPS provides an independent monitor of the overall power condition on the spacecraft and has the ability to reset, recycle, or cut power to the remainder of the spacecraft upon detection of warnings, errors, or anomalies. The EPS maintains a nominal 8V battery bus, and provides conditioned 5 and 3.3V lines off of the battery bus. The EPS generates an average of 1.8W when the DICE sensor-sats are oriented in their final spin state around the Z-axis aligned with the geodetic axis.

### *DICE Attitude Determination and Control Systems*

ADCS on DICE is handled by both the C&DH PIC24 microcontroller and a Micromega floating point unit (FPU) on the ADCS board. Data is acquired for the ADCS algorithms via the ADCS electronics PCB, and includes 3-axis magnetometer, sun sensor vector, and GPS position and velocity measurements. The torque coil drive circuitis are also located on the ADCS electronics PCB. Because the C&DH PIC24 is inefficient at calculating floating-point numbers, the FPU receives data and instructions from the PIC24, performs the calculations, and returns the results. The magnetometer and sun sensor are sampled by the data acquisition manager task every 10 Hz to feed the ADCS algorithms. The returned results are then used for pulse-width modulation firing of the torque coils. The various DICE ADCS algorithm and state definitions and associated parameters are shown in Panel 1.

The DICE ADCS operates in two states. The first state, Detumble, is entered upon power up of the spacecraft. The spacecraft will remain in this state permanently until commanded from the ground to do otherwise.

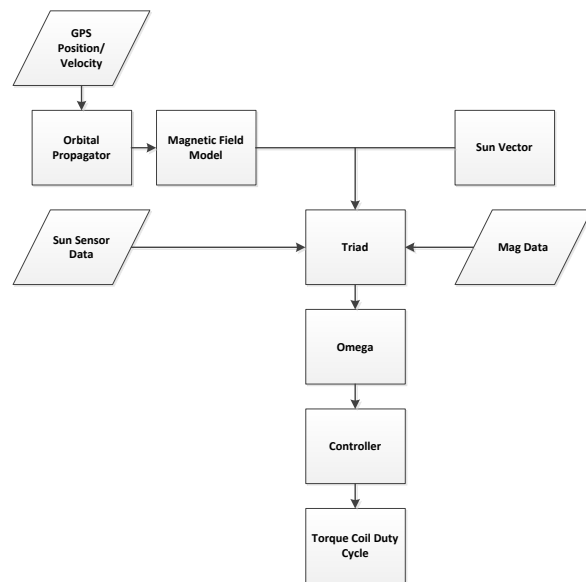


**Figure 10. Data flow and events diagram for the DICE ADCS Controller state.**

Upon receiving command from the ground, DICE enters into its Controller state. In Detumble state, based upon magnetometer measurements the spacecraft will “slow” the X and Y axes motion (in regards to the spin rate) and begin to spin up the Z axis in preparation to operate in the Controller state where the spacecraft will maintain the desired spin rate as controlled by ground

commands as well as alignment with the geodetic axis. Sun sensor and magnetometer measurements are used in the Controller state. The interaction of inputs, outputs, and ADCS algorithms for the Controller state is shown in Figure 10.

Each DICE spacecraft carries a NovAtel OEMV-1 GPS receiver along with a commercial L1 patch antenna placed on the +Z top plate of spacecraft. As the spacecraft spins about its Z axis at up to 2Hz, the patch antenna rotates but maintains the same GPS constellation vehicles in view for several minutes allowing the receiver to acquire the signals long enough to produce a position and velocity solution. Due to the 916mW power consumption of the GPS and antenna, these devices are only powered on periodically (nominally every 3 hours) and powered down after the solution is acquired.

Pre-flight testing of the OEMV-1 using the NASA Goddard Space Flight Center GPS simulator was performed using a variety of spacecraft attitude scenarios including insertion tumbling after deployment, insertion orbit 0.1Hz and 1Hz spin with geodetic axis alignment, as well as end of life orbit 1Hz spin with geodetic axis alignment. While acquiring a consistent lock and position solution in the tumble scenario was challenging, consistent locks could be made in all other scenarios regardless of spacecraft altitude or spin rate, with time-to-lock from cold start ranging from 75 to 810 seconds and an average of 401 seconds. An interesting correlation was observed for all scenarios involving spin about the spacecraft axis when is aligned to the geodetic axis. Locks tended to acquire more quickly when cold start was initiated as the spacecraft entered low latitudes (lower than -45 degrees) as shown in Figure 11.

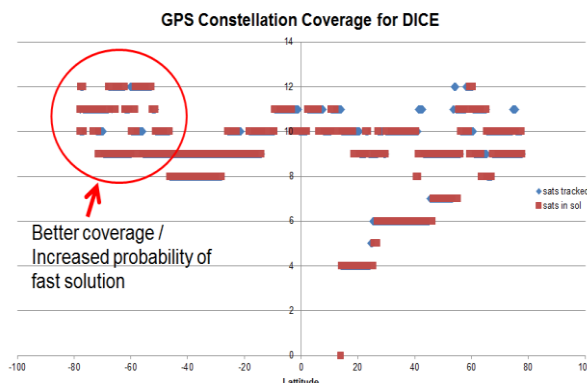


**Figure 11. GPS simulation test data from NASA Goddard. In this data set, the DICE spacecraft were aligned with the geodetic axis and spinning.**

DICE implements a precise clock which tracks real time to < 90 ns precision in the science payload electronics FPGA. Clock drift is corrected and synchronized by the C&DH whenever the GPS receiver is powered on and producing precise time solutions, as shown in Figure 12. The DICE-time synchronization scheme allows the payload clock to be synchronized to the GPS receiver's clock to within 250 ns or within 270 ns of real time. Emulated GPS time stamps can also be sent from the ground to the spacecraft during mission operation times in which the GPS is not powered on and acquiring real GPS time, position, and velocity. Time accuracy is degraded during these times.

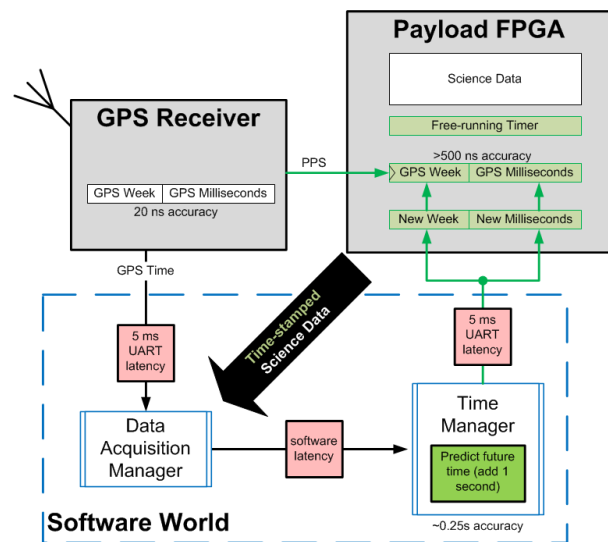


**Figure 12. The DICE system timing is based on a combination of clocks that are ultimately synchronized to GPS time.**

### Communications and Ground Stations

The on-board data acquisition rate of each DICE sensor-sat is > 10 kBits/second when in science mode. To store and forward transmit this data to the ground from the DICE constellation at an on average daily cadence requires an on-board storage of ~ 1 Gbit/day and a downlink rate greater than 1.5 Mbits/second (assumes approximately 7-10 minutes of overpass downlink time per sensor-sat per day). The on-board storage requirement is well within typical CubeSat technology specifications. However, the downlink rates are much greater (by a factor of 100-200) than those used on most previous CubeSat missions. Prior CubeSat missions have typically been “beacon” communicators that relied on amateur radio frequencies for downlink communications as well as enthusiastic amateur radio operator interest to track the spacecraft, acquire the beacon data, and then distribute the mission data to those interested. Additionally, as DICE was sponsored

by NSF and NASA and it fundamentally falls into a mission type that should be using communication bands associated with government activities.

Therefore, in collaboration with L-3 Communications, our team developed the Cadet U CubeSat radio to enable high downlink data rates and to operate in the regulated UHF bands for both uplink and downlink.



**Figure 13.** L-3 Comm's Cadet U miniature radio is ideal for CubeSats and small satellites.

Each DICE spacecraft contains a Cadet U radio. The DICE ground station uses a GNU radio based software defined radio. The Cadet U is a 6.9 x 6.9 x 1.3 cm half-duplex modem, weighing only 0.08 kg, and capable of 9600 kbps uplink (450 MHz) and 20 Mbits/s of FEC encoded downlink (460-470 MHz). The DICE Cadet U radios downlink at 3 Mbits/s. The uplink is FSK modulated, while the downlink is OQPSK modulated. The Cadet U implements a store-and-forward architecture where data is continuously streamed to it from the C&DH through a simple UART. It is then pre-encoded and stored in the on board 4 GByte FLASH memory. Ground station operators have control over data transmission, data priority order, and how and when that data is deleted. Normal continuous receive operations consume ~ 200 mW, while transmission consumes ~9 W of power to produce up to 2 W of RF output power. Output power levels are selectable in 3dB increments. The uplink and downlink frequencies can be modified via ground commands. The Cadet U implements a custom command protocol which is essentially identical from the front end (RF from ground) or back end (UART to C&DH). The DICE spacecraft communicate with the ground stations using the CCSDS space packet protocol.

The DICE ground station utilizes an open-source software defined radio. Uplink commands and data requests are sent through a TI CC1101-based transmitter. Downlinks from the Cadet U are captured by the Ettus USRP2 which is hardware that has been specialized for software defined radios. These devices interface through a standard gigabit Ethernet NIC. Using GNU Radio, an open-source software readily available to the public, an interface is created and used to store data from the transmission at 10 Msamples/s. Upon completion of an overpass, data is run through a series of signal processing, demodulation, and FEC

decoding scripts before final ingesting into the data center database as level 0 data.

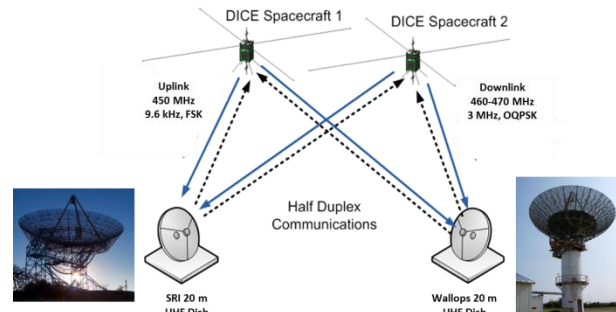


**Figure 14.** The DICE communications scenario utilizes the large UHF dishes at WFF and SRI to close the DICE high speed downlink.

To close the high speed downlink, the primary DICE mission ground station (GS) located at NASA Wallops Flight Facility (WFF), utilizes the software defined radio equipment in combination with the WFF 20 m (~ 35 dB gain) UHF dish. The secondary GS node is located at SRI International and uses a second DICE software defined radio in combination with their 20 m UHF dish. The DICE communications scenario schematic is shown in the Figure 14.

Student and professional staff at the USU/SDL DICE mission operations center (MOC) run the GSs remotely and coordinate operations with ASTRA. The DICE mission operations center (MOC) shown in Figure 15, remotely interfaces with the WFF and SRI GSs. The



**Figure 15.** The DICE MOC is run by students at USU/SDL.

MOC and GSs rely on the USAF Space Command's published orbital elements for satellite tracking. Spacecraft command and telemetry planning occurs during the week prior to scheduled activity. The USU/SDL MOC is connected to USU/SDL's gigabit intranet, facilitating preprocessing, archiving, and disseminating the mission's data products to the science team. USU/SDL maintains a data center (DC), managed by professionals and staffed by students. Daily data GS data acquisitions are ingested into and stored in a MySQL database that contains Level 0 to Level 3 data. The DC is



protected against power anomalies, fire, and other adversities. Data stored in the DC is regularly archived and stored at an off-site location. The DC furnishes secure communication for the DICE engineering and science teams, as well as public servers for the dissemination of mission data.

Table 2. DICE Data Products		
Data Product	Public Access Location	Data Elements
L0	USU/SDL ASTRA [MOC/DC]	<ul style="list-style-type: none"> <li>•Removal of duplicate data</li> <li>•Separation of bus &amp; science data</li> <li>•Correlation of system &amp; absolute time</li> </ul>
L1	USU/SDL ASTRA [MOC/DC]	<ul style="list-style-type: none"> <li>•Application of sensor calibration.</li> <li>•Insertion of orbital elements into data</li> <li>•Calculation of time/geodetic position</li> </ul>
L3	ASTRA	For selected storms: <ul style="list-style-type: none"> <li>• AMIE potential distribution</li> <li>• TIMEGCM fields (Ne, E-field, winds)</li> <li>• IDA4D Ne distribution</li> </ul>
Archive	USU/SDL [MOC/DC]	•Permanent archival of all mission data

The individual tasks that will be accomplished in Level 0–2 processing are outlined in Table 2. The DICE spacecraft data received by the MOC will be processed to Level 0 and then transferred to the DC for permanent storage and future access for higher level data product processing. ASTRA, USU/SDL, and Embry-Riddle will perform higher level data analysis. ASTRA also validates L0 and L1 data. USU/SDL and Embry-Riddle will provide the necessary algorithms for calibration of sensor data. ASTRA will run AMIE, TIMEGCM and IDA4D for selected storms during the mission. The model output will provide a framework for the interpretation of the DICE data<sup>13</sup>. AMIE and IDA4D will be run both with and without the DICE data, for comparison. ASTRA will be the public interface to the DICE higher level data.

## TEST AND CALIBRATION

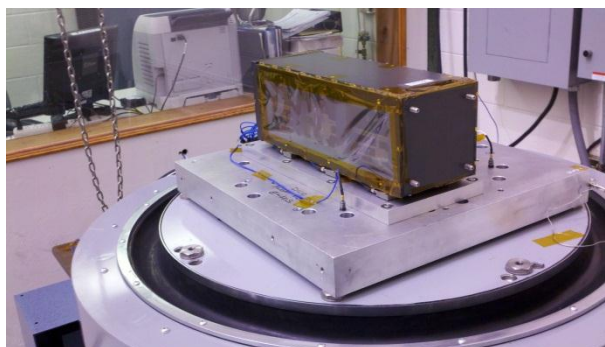


**Figure 16. DICE structural random vibration and sinusoidal survey testing.**

As part of the NASA ELaNa III program, the DICE spacecraft were required to undergo environmental qualification and launch specific functional testing. This testing focused on P-POD integrated testing and verification. Essentially, the integrated DICE P-POD assembly was required to demonstrate that there would not be any radio frequency, electrical, or structural interference between DICE and the host launch vehicle during launch as well as ~ one hour following ejection of DICE from the P-POD.

Environmental testing included 1) structural random vibration, sinusoidal survey (see Figure 16), and shock, and 2) thermal cycling and thermal vacuum bakeout. The majority of the environmental testing occurred at USU/SDL, which has a wide range of environmental test facilities that have been developed and used on many space flight programs over the past five decades. However, to perform the structural shock testing, USU/SDL teamed with ATK and used their shock test facilities located in Promontory, Utah.

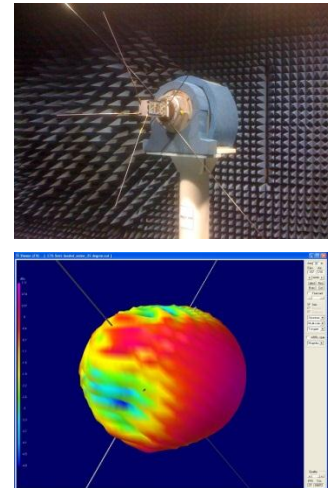


**Figure 17. Top Panel) The DICE antenna testing at NASA WFF. Bottom Panel) The resultant antenna pattern is fairly uniform over all view angles (pattern is from a simulated model that closely matches the WFF test data).**

Non-ELaNa mission functional testing included “day in the life” operations verification, communication link budget and antenna pattern verification, mass properties verification, ADCS algorithm performance verification, and EPS performance verification testing. The communication link budget and antenna pattern verification occurred in collaboration with and at NASA WFF (see Figure 17). Additionally, USU/SDL has recently developed the Nano-satellite Operation Verification and Assessment (NOVA) facility (reference Figure 18), which was critical to the functional and mass properties testing on DICE. The NOVA facility includes access to a walk-in Helmholtz cage, NIST traceable solar simulator, inertia and mass properties tables, Gauss chamber, and other hardware-in-the-loop utilities. This CubeSat targeted test facility, along with the relative ease in handling CubeSat sized spacecraft, enabled quick turnaround testing and verification throughout the program.



**Figure 18. The USU/SDL NOVA test facility is specially designed to allow for easy access and quick turnaround for CubeSat sized functional testing and system performance calibration activities.**

Calibration of the science sensors was accomplished by examining the response of the sensors to known loads and test conditions. These measurements and analyses are performed both for bench-test scenarios, and while the sensors are undergoing thermal vacuum testing. Engineering quantities are related to digital counts by a set of polynomial coefficients according to

$$y = A_0 + A_1x + A_2x^2 + \dots \quad (1)$$

where  $y$  is the calibrated quantity (volts, amperes, degrees, etc.) and  $x$  is the telemetered integer quantity. Several of the calibrations were found to depend significantly on temperature; so the coefficients,  $A_i$ , will vary according to temperature. Therefore, the conversion from counts to engineering units for these values is a two-step process. First, the  $A$  coefficients are obtained by using the appropriate housekeeping temperature monitor according to

$$A_0 = b_0 + m_0T \quad (2)$$

$$A_1 = b_1 + m_1T \quad (3)$$

where  $T$  is the measured temperature, and the coefficients  $b$  and  $m$  are determined during thermal vacuum testing and calibration. Once the coefficients  $A$  are determined, then the conversion from counts ( $x$ ) to engineering quantities ( $y$ ) is performed.

The electric field sensor is treated as a voltmeter. A stable voltage source was applied between the differential probe surfaces and measured with a calibrated voltmeter. The measured voltage and the telemetered counts were used to obtain the correct

calibration coefficients. The magnetometer was calibrated in a characterized Helmholtz coil located within a Gauss chamber, with triple-walled Mu-metal. The Helmholtz coil was driven with known currents as measured by a calibrated ammeter. The Langmuir probes were treated as ammeters and varying known resistive loads were applied to their sensor outputs. The measured current readings and the telemetered counts were used to obtain the correct calibration coefficients. These calibrations were performed over a range of temperatures during bench top and thermal chamber testing.

Figure 19 is a plot of the residuals of a linear result from the calibration process of electric field data. Figure 20 shows plots of the nine elements the final calibration matrix for the 3-axis magnetometer data.

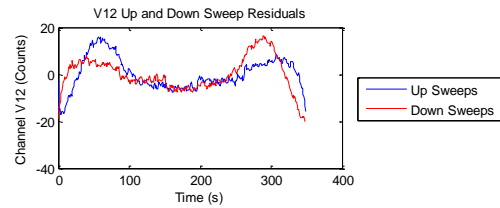


**Figure 19. Calibration data residuals from triangle wave inputs to the electric field sensor.**

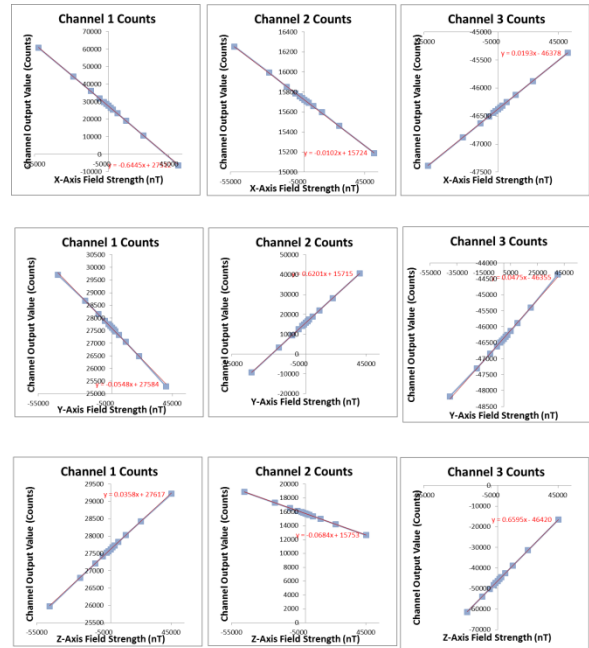


**Figure 20. Calibrated data for the DICE 3-axis magnetoreactive science magnetometers.**

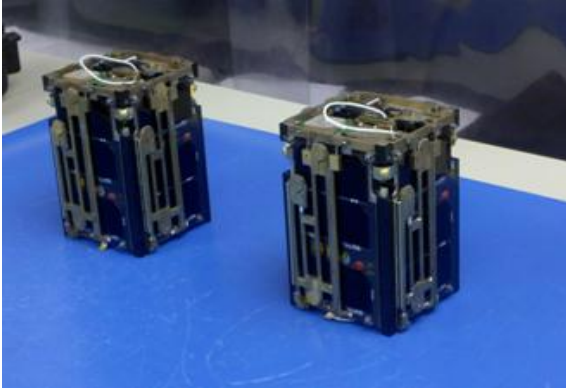


Figure 21. The DICE spacecraft, Farkle and Yahtzee, prior to integration into the launch P-POD.



Figure 22. The DICE spacecraft were launched as secondary payloads out of Vandenberg AFB on Oct. 28, 2011 as part of the NASA ELaNa III program.

## ON ORBIT OPERATIONS AND PERFORMANCE

### *Launch and Early Operations*

DICE was successfully launched as part of the NASA ELaNa III program as a secondary payload out of Vandenberg AFB on the Joint Polar Satellite System NPOESS Preparatory Project launch on October 28, 2011. The two spacecraft were launched unpowered and ejected from the same 3U P-POD; Farkle saw first light followed very shortly by Yahtzee. The two were ejected with a few cm/s of relative velocity difference to introduce a gradual separation, enabling both close proximity and large distance trailing measurements over varying times of the mission. The orbit insertion information is shown in Table 3.

Following ejection from the P-POD, both DICE spacecraft powered on and entered Survival mode. A 50 minute timer was also initiated. After 50 minutes, the spacecraft main mechanism release subsystem was automatically activated, firing the miniature TiNi

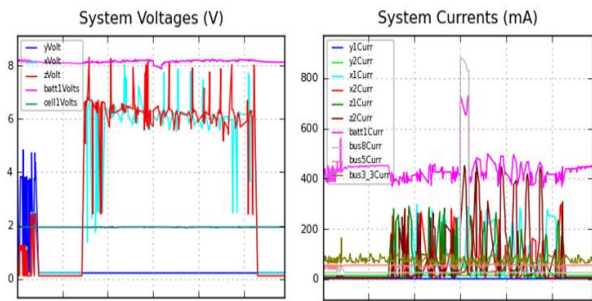


Figure 23. DICE sensor-sat housekeeping telemetry following launch and ejection into orbit from the PPOD. The initial data on the left in the plot is from ground testing that was intentionally kept in the on-board memory during launch. That is followed by voltage and currents captured after ejection into eclipse. That is then followed by the sensor-sat's first view of the sun, at which point the solar panel voltages and currents become active. The spike seen in the current about half-way through the first solar viewing is due to the firing of the DICE antenna and Langmuir boom mechanism release actuator. Housekeeping data is acquired at a 0.1 Hz nominal rate onboard the spacecraft, leaving a significant majority of the telemetry on-board storage and transmitted bandwidth for the science measurements.

Table 3. DICE Spacecraft Orbit Insertion Parameters

S/C	Period (min)	Inclination (°)	Apogee (km)	Perigee (km)
Farkle	97.35	101.72	808	456
Yahtzee	97.34	101.72	807	456

Frangibolt, after which the antenna and Langmuir probe booms were deployed. The electric field booms were not deployed at this time. These events, as recorded in the DICE housekeeping data, is shown in Figure 23.

Within ~ two weeks following launch, both spacecraft were put into Standby mode and the spacecraft were detumbled to a few degrees per second per axis rotation rates. At this point, both spacecraft began nominal on-orbit maintenance and communication operations.

### *Nominal Operations*

Both DICE spacecraft have been operating continuously since October 2011. Orbital elements have been refined and tracking and communications (9.6 Kb/s uplink, 3 Mb/s downlink) with both spacecraft out



of WFF and SRI have occurred regularly during that period. Contacts occur every Monday through Friday from WFF. The original DICE baseline on-orbit mission duration was planned for 90 days, however it is expected that the DICE mission can operate for an additional 3 years, limited by battery degradation.

All sub-systems have demonstrated operational functionality. Figure 24 shows housekeeping data, including spacecraft temperatures EPS voltage and current readings. Figure 24 also shows ADCS sun sensor measurements errors, which are well below expected levels.

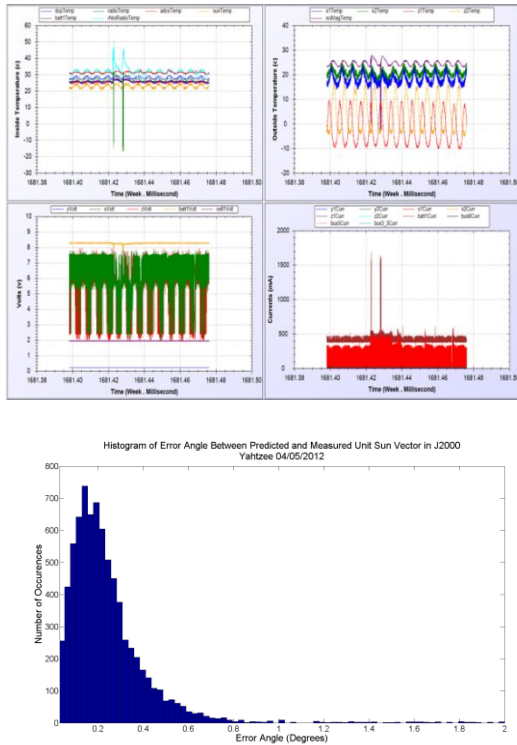


**Figure 24. Top Panel) DICE housekeeping data. The two top plots are of spacecraft temperatures. The larger swing temperatures in the top right plot are from the solar panels which are thermally isolated from the rest of the structure. The bottom left panel demonstrates the ~8V battery bus maintained by the EPS. The spikes in temperature and current (most notable in the top left and bottom left plots) are during times of downlink transmission when the radio is in high power mode. This data covers ~13 orbits in time. Bottom Panel) DICE sun sensor measurements demonstrating on-orbit average pointing error knowledge of  $< 0.3^\circ$ .**

Figure 25 shows measurements from the Langmuir and science magnetometer sensors. The science sensor measurements exhibit agreement with established ionospheric model predictions, while also demonstrating fine structure detail not expected from the models. The electric field sensors are also acquiring data, however the electric field wire booms have not been deployed as of yet so the electric field sensor spheres continue grounded (stowed configuration) to the spacecraft structures.

Deployment of the electric field wire booms are the next step in the DICE on-orbit operations process. This

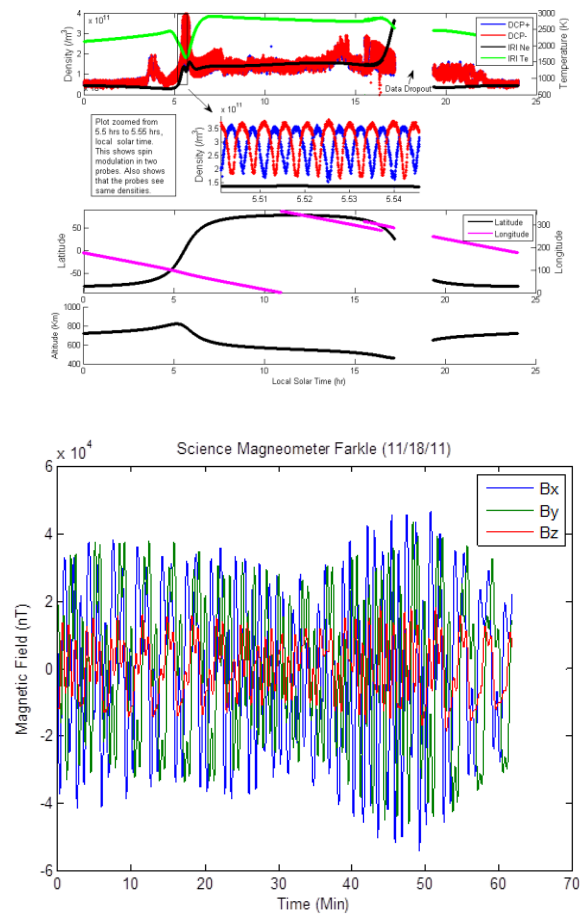


**Figure 25. Top Panel) Data from one of the two DICE 1.5U CubeSats. Both fixed bias Langmuir probes track each other. While they also generally agree with IRI structure, they also show unique structure seen in-situ. They also show spin modulation due to the spacecraft being in a slow detumble state. Bottom Panel) Science magnetometer data from early in the mission.**



process will include a final orientation of the spacecraft Z axis (long axis of the spacecraft) with the geodetic axis (reference Figure 26). Initially, the spacecraft will be spun up to  $\sim 2$  Hz around the Z axis to deploy the booms. The final spin rate, following the 5 m wire boom deployments, is expected to be  $\sim 0.1$  Hz. Electric field measurements will be made throughout this event to fully characterize the boom deployment process.

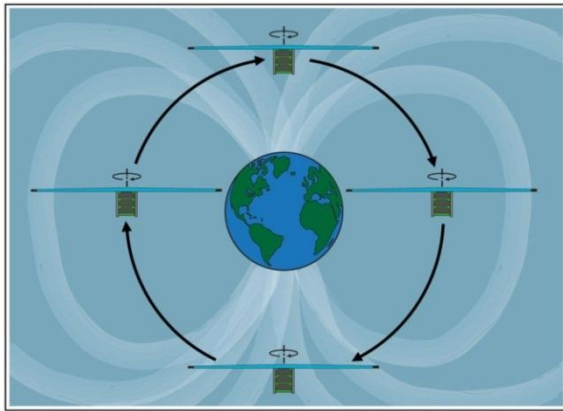


**Figure 26. DICE sensor-sat orbital orientation in final spin up state.**

The spacecraft spin stabilization will provide two-dimensional measurements of the electric field, and thus allow a deterministic ground processing removal of the  $\mathbf{v} \times \mathbf{B}$  induced electric field component that is superimposed upon the target environmental electric field due to spacecraft movement through the geomagnetic field. The worst case  $\mathbf{v} \times \mathbf{B}$  induced electric field component is expected to be on the order of 350 mV/m, while the quiet time environmental EFP measurement capability is expected to be on the order of 0.5 mV/m. Therefore, the process of systematically determining the  $\mathbf{v} \times \mathbf{B}$  electric field from the sinusoidal measurement created by the spin of the spacecraft is critical in removing the induced field component from the total measurement during data analysis. In addition, accurate knowledge of the spacecraft attitude (within  $1^\circ$ ,  $1\sigma$ ) is important in determining the contribution of the induced field to the total measurement. The minimum electric field measurement capability of 0.5 mV/m is a typical equatorial quiet time value. Storm-time electric fields associated with SEDs are several times larger. The 0.5 mV/m measurement threshold is limited by such features as the sensor surface work function and the local environment created by the wake of the spacecraft. Thus, the electric field wire booms have been designed to extend to distances much greater than the spacecraft structure size. While the electric field threshold is conservatively expected to be 0.5

mV/m, the resolution is much finer at 100  $\mu$ V/m. Post-mission processing may enable a threshold smaller than 0.5 mV/m to be obtained.

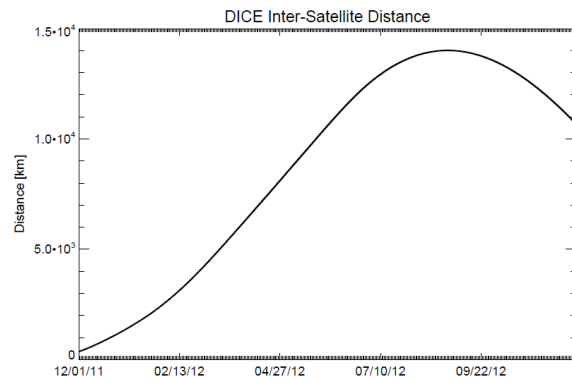


**Figure 27. The DICE sensor-sats have been gradually separating since mission launch.**

It is expected that each DICE spacecraft will spin with the spacecraft Z axis aligned to  $\leq 5^\circ$  ( $1\sigma$ ) of the inertial J2000 z-axis. As discussed, this orbital orientation facilitates the measurement of the electric field component orthogonal to the geomagnetic field over a majority of the orbit but additionally, this orbital orientation ensures a purely spherical projection of the DCP sphere into the spacecraft ram direction with only minor effect from the cylindrical boom at high latitudes. It is expected that post-processing will determine spacecraft attitude to much less than  $1^\circ$  ( $1\sigma$ , 3-axis).

The progression of the relative separation of the DICE sensor-sats is shown in Figure 27. This slow separation (and approach – starting again later this year) has allowed for study of ionospheric events with varying temporal and spatial characteristics. This process will continue over the life of DICE. Additionally, the DICE orbits continue to precess and move in and out of prime SED coverage. The first prime SED science window occurred shortly after launch, with (see Figure 28 top panel) with future windows cycling into DICE's view  $\sim$  every seven months.

### Communications

There has been a tremendous improvement in the amount of downlinked DICE data that can be demodulated and decoded by the software defined radio since the inception of the program. The first set of DICE telemetry was demodulated and decoded at  $\sim$  a 10% success level. However, as of the writing of this paper, that success level has increased to a consistent 90-100%. The change in successful demodulation and

decoding and final ingestion of the data in to the DC is due to a number of key changes in the hardware and software components of the software defined radio, as well as changes in operational communication bands. The uplink communications have been fully functional at a 100% success level since launch.

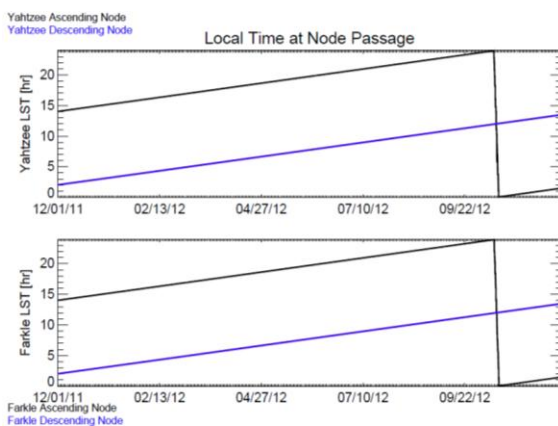
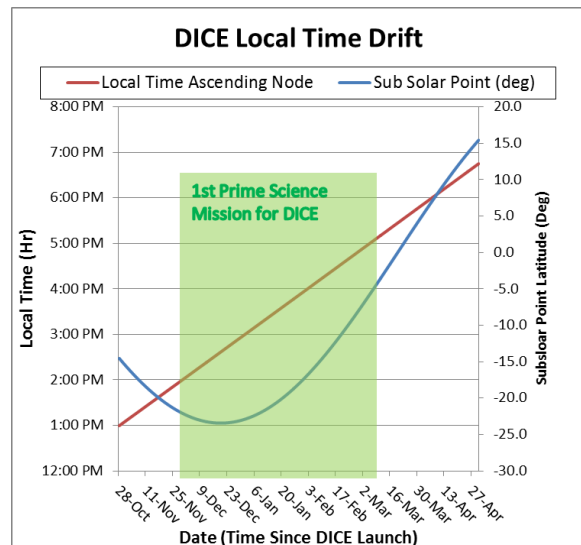


**Figure 28.** The DICE prime-time science windows are between 1400-1700 LT. Top Panel) Definition of first window. Bottom Panel) The DICE sensor-sats will cycle through the prime-time science windows ~ every 7 months.

DICE downlink communications began centered at 465 MHz. Site surveys at WFF and SRI prior to launch indicated that the 468 MHz band was spectrally cleaner, but a miscommunication during the formal frequency operation request process resulted in a 465 MHz approval. However, DICE was also formally recognized as being able to operate over the entire 460-470 MHz

space to earth spectrum during the frequency operation request process; thus, given appropriate approval, DICE could move to other center bands of operation in the 460-470 MHz spectrum if needed. It was quickly determined that a change would be needed. As the 460-470 MHz space to earth spectrum is a secondary user role, DICE downlink transmissions were consistently competing with noise and chatter due to local ground communication (e.g., police and government activities, pager systems, etc.). It was quickly determined through daily operations that centering around 468 MHz would give DICE a much quieter, although not completely silent, center band of operation for its  $\sim \pm 1.5$  MHz of required bandwidth.

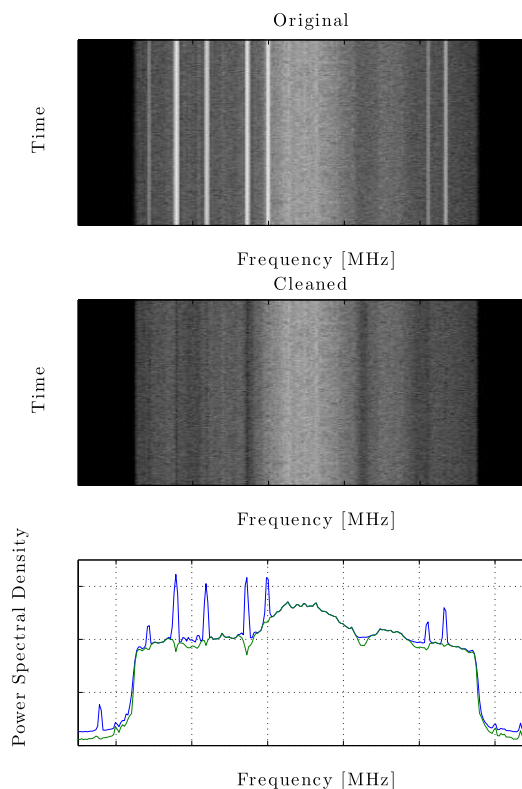


**Figure 29.** The DICE team developed signal processing code to scrub the noisy data, centered at 465 MHz, and remove the competing local chatter that interferes with the desired DICE spectrum. In the bottom plot, the green spectrum profile is what is left after the “cleaning” process has occurred (correlates with middle plot).

A formal request was made to change the DICE center band of operation to 468 MHz. However, in addition to this operational change, the DICE team made significant improvements in both the hardware and software aspects of the software defined radio GS. First,

in collaboration with RF engineers at WFF, we developed a very sharply filtered low-noise amplifier for 468 MHz operation to go on the front of the USRP2 receiver input. The prior design was a much wider band implementation. Second, the DICE software defined radio team developed new signal processing techniques to remove a large portion of the interference, while still allowing for detection, demodulation, and decoding of the resultant DICE data. An example of this “cleaning” process is shown in Figure 29.

The formal approval to operate at 468 MHz occurred in May 2012. The DICE spacecraft were commanded to downlink at this frequency, the WFF filter and low-noise amplifier were put in place, and the new software defined radio signal processing techniques were included in the code set of the GS. A combination of these pieces, as well as other refinements of the software defined radio code, has increased our DICE data capture level from a mere 10% to nearly 100% for all downlinks.

Due to high levels of tracking performance from the GSs at WFF and SRI, and the nearly isotropic DICE spacecraft antenna pattern, DICE earth to space and space to earth communications quite often occur from horizon to horizon (0 to 0°). We are able to close uplink and downlink paths frequently at ranges > 3000 km. And when we are in 24/7 mini-campaign operation mode with both WFF and SRI GSs, ~ 90 minutes of high reliability DICE communications can be executed over a the course of a day.

## LESSONS LEARNED

Given the very low budget pathfinder and educational nature of the DICE mission, a number of lessons learned were expected. There were of course the common lessons learned that are applicable to most space flight programs, such as the desire to have budgeted and tracked programmatic and technical resources more resolutely to have enabled greater test (and retest) time on the fully integrated system, as well as additional time to comprehensively test sub-components before integration into the complete system. However, the DICE team feels that there are a number of other lessons learned that might be unique to DICE or the NSF CubeSat program that are worth sharing with the community in hopes of helping positively push forward the great CubeSat-based space research and operations revolution that is advancing at such an unexpected accelerating pace:

### *Programmatic*

1. Great things can indeed come from humble settings. While the funding allocated to the

NSF CubeSat programs is miniscule in comparison to most other government sponsored space flight programs with similar expectations, the leeway given to the PI and professional and student teams to implement the mission encourages incredible resourcefulness and efficient use of program resources.

2. Positive collaboration between government, academia, small business, and industry with a set of common goals can be very productive in developing far reaching space mission technologies and processes at very low cost and impact. The DICE team was immensely benefited by collaboration and contributions from L-3 Communications, TiNi Aerospace, ATK, WFF, and SRI. Very high-speed space to earth communications, miniature reliable actuators, and high end software defined radios for GSs were developed through our collaborations and teaming.
3. The support of NASA ELaNa in providing launch services to the CubeSat community is invaluable in the sense that it allows the individual mission teams to focus on spacecraft, sensor, and mission operations development. The coordination of launch integration is a very large task and the removal of that burden from the NSF CubeSat program mission teams has a very positive impact.

### *Technical*

1. While the development and assembly of small CubeSats can be much easier and quicker than larger spacecraft, the on-orbit spacecraft operations and management of the downlinked data is equivalent in scope to traditional missions. Once the CubeSats have reached orbit, all semblances of “smallness” disappear. Thus, the approach for management of research and operational CubeSat missions needs to be considered in respect to traditional mission approaches.
2. The engineering challenge of producing well performing science instruments within the technical resource constraints of a Cubesat is every bit as valuable as seeing how big we can make our farthest seeing large telescopes. Pushing the frontiers of technology is invaluable to our future progress and competitiveness.
3. NSF and NASA-sponsored CubeSat programs in general can greatly benefit by using government requested communication bands and established GS sites at WFF, SRI, and potentially other facilities such as Morehead

State. This does not exclude use of the amateur community infrastructure (e.g., use of beacons on CubeSats), but it does encourage regular research and operations classification of future government sponsored CubeSat programs and allows the CubeSat community to take advantage of the great amount of engineering that has already occurred in developing the larger GS facilities.

4. CubeSats should, and will be, the backbone of many future global multi-point measurement missions (and not just for geospace!). Pushing from the CubeSat end of the size spectrum has opened up many new paths to low cost, easier access to space for upcoming constellation missions.

## ACKNOWLEDGMENTS

The authors gratefully acknowledge funding provided by NSF [grant numbers# ATM-0838059, AGS-1212381], to the NASA ELaNa III group for launch services provided for the DICE program, and to NASA WFF for their professionalism and willingness to help DICE succeed. The authors also gratefully acknowledge the countless hours of dedicated and passionate effort from the students on the DICE program. They indeed rose to the challenge and gave much more than was ever expected of them. Without their energy and consistency, DICE would not have become a reality.

## REFERENCES

1. Heliophysics The Solar and Space Physics of a New Era, Recommended Roadmap for Science and Technology 2009-2030, NASA, May 2009
2. Skone, S., M. El-Gizawy, and S. M. Shrestha, (2004), Analysis of differential GPS performance for marine users during solar maximum, *Radio Sci.*, 39, RS1S17, doi:10.1029/2002RS002884
3. Sojka, J. J., D. Rice, J. V. Eccles, F. T. Berkey, P. Kintner, and W. Denig (2004), Understanding midlatitude spaceweather: Storm impacts observed at Bear Lake Observatory on 31 March 2001, *Space Weather*, 2, S10006, doi:10.1029/2004SW000086.
4. Foster, J. C. (1993), Storm time plasma transport at middle and high latitudes, *J. Geophys. Res.*, 98, 1675.
5. Klobuchar, J. A., J. Aarons, and H. H. Hosseinich (1968), Midlatitude nighttime total electron content behavior during magnetically disturbed periods, *J. Geophys. Res.*, 73, 7530–7534.
6. Mendillo, M. (2006), Storms in the ionosphere: Patterns and processes for total electron content, *Rev. Geophys.*, 44, RG4001, doi:10.1029/2005RG000193.
7. Coster, A. J., J. Foster, and P. Erickson, Monitoring the Ionosphere with GPS: *Space Weather*, GPS World, 14(5), 42-49, 2003.
8. Foster, J. C., and W. Rideout (2005), Midlatitude TEC enhancements during the October 2003 superstorm, *Geophys. Res. Lett.*, 32, L12S04, 10.1029/2004GL021719
9. Foster, J. C., and A.J. Coster, (2007), Conjugate localized enhancement of total electron content at low latitudes in the American sector, *Journal of Atmospheric and Solar-Terrestrial Physics* 69 (2007) 1241–1252, doi:10.1016/j.jastp.2006.09.012
10. Mannucci, Tsurutani, Abdu, Gonzales, Komjathy, Iijima, Crowley and Anderson, “Superposed Epoch Analysis Of The Ionospheric Response To Four Intense Geomagnetic Storms”, submitted to *J. Geophys. Res.*, August 2007
11. Foster, J. C., and H. B. Vo, Average characteristics and activity dependence of the subauroral polarization stream, *J. Geophys. Res.*, 107(A12), 1475, doi:10.1029/2002JA009409, 2002.
12. Foster J.C., P. J. Erickson, F.D. Lind, and W. Rideout (2004), Millstone Hill coherent-scatter radar observations of electric field variability in the sub-auroral polarization stream, *Geophys. Res. Lett.*, 31, L21803, doi:10.1029/2004GL021271
13. Crowley, G., C. Hackert, R. R. Meier, D. J. Strickland, L. J. Paxton, X. Pi, A. Manucci, A. Christensen, D. Morrison, G. Bust, R. G. Roble, N. Curtis, G. Wene, Global Thermosphere-Ionosphere Response to Onset of November 20, 2003 Magnetic Storm, *J. Geophys. Res.*, 111, A10S18, doi:10.1029/2005JA011518, 2006.
14. Crowley, G., C. Fish, C. Swenson, R. Burt, T. Nielsen, A. Barjatya, G. Bust, and M. Larsen, Dynamic Ionosphere CubeSat Experiment (DICE), Paper # SSC10-III-7, Proceedings of Small Sat Conference, Logan, UT 2010
15. Crowley, G., C. Fish, C. Swenson, R. Burt, E. Stromberg, T. Nielsen, S. Burr, A. Barjatya, G. Bust, and M. Larsen, Dynamic Ionosphere CubeSat Experiment (DICE), Paper # SSC11-XII-6, Proceedings of Small Sat Conference, Logan, UT 2011